KFBD

Araştırma Makalesi / Research Article

Investigation Of Some Optical And Electrical Properties Of InSe Thin Film, a Window Layer for Photovoltaic Cell Growth on Glass/GaSe Substrate by M-CBD Method

Fatih ÜNAL[1*]

Abstract

The InSe thin film was successfully grown on a glass/GaSe substrate using the modified chemical bath deposition (M-CBD) method and a group was annealed one hour at 80 °C in atmospheric conditions. The energy band gap (Eg) values of the as-deposited and annealed films were defined 1,89 eV and 1,15 eV, respectively. The transmitance values (%) of the as-deposited and annealed films were asigned %0.65, %4.46 and %11,02, %10,35 at 400 and 700 nm, respectively. The I-V characteristics of the device at different temperatures was examined, the resistivity decreased and the conductivity increased with the increasing temperature. The activation energy in low temperature region was defined 0,05 eV, while it was defined 0.6 eV in high temperature region.

Keywords: InSe, GaSe, M-CBD, Thin film.

Fotovoltaik Hücrelerde Pencere Tabakası Olarak Kullanılan InSe İnce Filminin Cam/Gase Alt Tabanı Üzerine M-CBD Yöntemiyle Büyütülmesi ve Bazı Optiksel ve Elektriksel Özelliklerinin İncelenmesi

Öz

InSe ince filmi başarılı bir şekilde cam/GaSe alt tabanı üzerine modifiye edilmiş kimyasal banyo depolama (M-CBD) yöntemiyle büyütülmüştür ve üretilen filmlerin bir gurubu atmosfer ortamında bir saat 80 °C'de tavlanmıştır. Üretilen ve tavlanan filmlerin enerji band aralıkları sırasıyla 1,89 eV, 1,15 eV olarak belirlenmiştir. Üretilen ve tavlanan filmlerin 400-700 nm'de yüzde geçirgenlik değerleri sırasıyla %0.65, %4.46 ve %11,02, %10,35 olduğu görülmüştür. Farklı sıcaklıklarda ölçülen I-V krakterizasyonlarında sıcaklığın artmasıyla özdirencin azaldığı, iletkenliğin arttığı görülmüştür. Düşük sıcaklık bölgesinde aktivasyon enerjisi 0,05 eV iken, yüksek sıcaklık bölgesinde 0,6 eV olduğu gözlemlenmiştir.

Anahtar kelimeler: InSe, GaSe, M-CBD, İnce film.

[1]Giresun University, Central Research Laboratory Application And Research Center, Giresun, Türkiye, fatih.unal@giresun.edu.tr

[1]https://orcid.org/0000-0002-6155-7051

1. Introduction

In_xSe_y compound can be formed different atomic combination and phases like InSe, In_6Se_7 In_4Se_3, In_2Se_3, In_9Se_{11}, etc. have been confirmed as attractiving inorganic semiconductors during past few decades (Igasaki and Fujiwara 1996, Camara, Mauger et al. 2002, Camara, Mauger et al. 2002, Gopal, Viswanathan et al. 2004). Indium selenite (In_xSe_y) belong to A^{III}-B^{VI} group contains a layered structure similar to the GaS and GaSe compounds. This structure is bounded in two dimensions by covalent bonds and by Van der Waals forces in three dimensions (Choi and Yu 2003). Indium selenite, which can exhibit n-type, has direct band gap (Pathan, Kulkarni et al. 2005). They are of particular interest to researchers because of their remarkable optical and photophysical properties that are promising for capacitors, solar cells, field effect transistors, photovoltaics and a variety of nanoelectronic applications (Mudd, Svatek et al. 2013, Han, Chen et al. 2014, Yuksek, Yaglioglu et al. 2014, Ho and Chu 2015, Boukhvalov, Gurbulak et al. 2017, Politano, Campi et al. 2017, Zhou, Shi et al. 2018). It has been widely researched for its application especially in photovoltaic device fabrication (Gopal, Viswanathan et al. 2005). In_xSe_y has been used either as a windows layer (El-Sayed 2003) in CIS/In_xSe_y as well as an absorber layer (Julien, Chevy et al. 1990) in In_xSe_y/CdS solar cell. There are number of deposition techniques such as flash evaporation (Julien, Benramdane et al. 1990), molecular beam epitaxy (Zhou, Shi et al. 2018), chemical vapor deposition (Jin-Ho Park, Mohammad Afzaal et al. 2003), van der walls epitaxy (Lang, Klein et al. 1995) and vacuum evaporation (Gopal, Viswanathan et al. 2005) for preparation of In_xSe_y thin films. However, the modified chemical bath deposition (M-CBD) method is an simple, low temperature and inexpensive technique that could fabricate films with high quality for device applications such as heterojunction devices, switching etc. (Lokhande and Pawar 1989).

In this study, we have coated the InSe semiconductor on glass/GaSe thin film substrate for M-CBD method and examined its optical and electrical properties. It is aimed to synthesize glass/GaSe/InSe heterojunction at low cost, examine their optical and electrical properties, and as a result, to present them as an alternative material that can be used in the construction of opto-electronic circuit elements.

2. Material and Methods

InSe thin films were deposited at room temperature on glass/GaSe(hexagonal) thin film substrate of 3x3 cm dimensions by M-CBD method. For cationic solutions, acidic (pH≈3) $In_2(SO_4)_3$ solutions of 0.07 M concentrations were used while for anionic ones, basic (pH≈12) Na_2SeSO_3 solution of 0.05 M was used.

The glass/GaSe substrates were 60 times immersed in $In_2(SO_4)_3$ precursor solution for 30 seconds, in distilled water for 70 seconds, in Na_2SeSO_3 precursor solution for 10 seconds and distilled water for 70 seconds respectively. The two of the fabricated films were also annealed at 80 °C temperatures in air atmosphere for one hour.

Optical properties were investigated by Perkin-Elmer Lambda 25 UV-Vis spectrophotometer. The I-V measurements were carried out with Keithley 6486 pico-amperometer and Pasco Scientific SF–9585 A power source using two probe technique in which silver metal was used for contacts.

3. Findings and Discussion

3.1 Optical Properties

The thickness of InSe thin film growth on glass/GaSe substrate in 60 steps was estimated to be 90 nm.

The optical absorbance and transmittance spectra against wavelength in the range 400 – 1100 nm at room temperature for glass/GaSe/InSe film is shown in Figure 1a and c, respectively. The graph of the absorption coefficient (α_a) versus photon energy is given in Figure 1b. The highest value of α_a is $9,3x10^6$ at 2,26 eV. As seen in Figure 1 a, the maximum absorption peak is 547 nm in the UV region and the absorption decreases with increasing wavelength. This behavior is a characteristic feature of existence of states with free carries that localized in the energy band gap (ÜNAL, İZGİ et al. 2020). Figure 1 c also plotted wavelength versus percent transmitance. Glass/GaSe/InSe thin film is highly transmitance at wavelengths greater than 700 nm but the transmittance value at 400 and 700 nm is %0.65, %4.46, respectively. These values are very low and mean that the glass/GaSe/InSe thin film is a good absorbent material at the visible region boundaries.

The basic absorption spectrum is one of the most used methods to determine the energy band gap (E_g). The relation between absorption coefficient and energy band gap is given (Tauc 1968)

$$\alpha(hv) \approx \left(hv - E_g\right)^n \qquad (1)$$

where α is the absorption coefficient and hv is the energy of absorbance light. The value of n is ½ for direct allowed transitions for InSe (Gopal, Viswanathan et al. 2005) materials. This method uses the plot of $(\alpha hv)^{\frac{1}{n}}$ versus hv (Figure 1 d). E_g is determined by extrapolating the straight line portion of this plot to the energy axis. The intercept on energy axis gives the value of E_g, and have yielded 1.89 eV. It is seen that the result obtained is lower than the energy band gaps of metal oxide semiconductor films(Dugan, Koç et al. 2020, Yetim, Aslan et al. 2020).
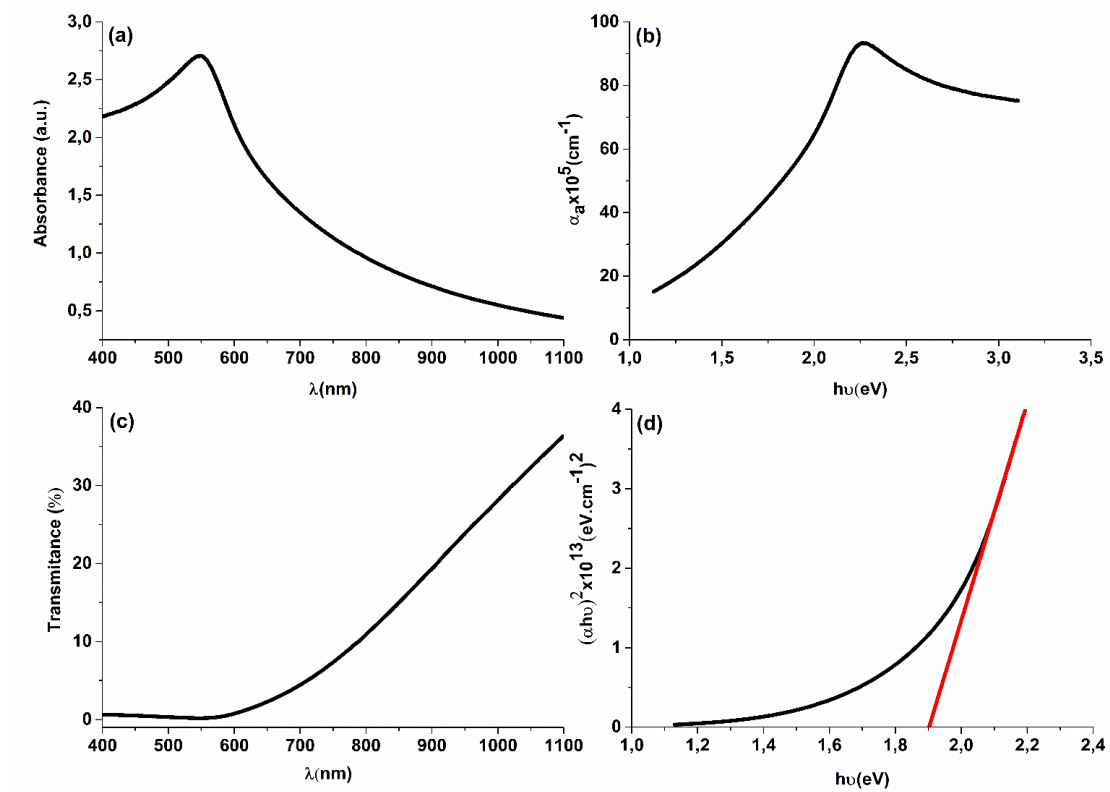
Figure 1. The optical spectrum of glass/GaSe/InSe thin films: a) absorbance, b) absorbtion coefficient, c) transmittance and d) the photon energy dependence of $(\alpha h\upsilon)^2$.

Optical absorption and transmittance plotted against the 400-1100 nm wavelength of glass/GaSe/InSe(annealed) thin film are given in Figure 2a and c, respectively. The absorption coefficient (α_a) and $(\alpha h\upsilon)^2$ plotted against photon energy are given in Figure 2b and d, respectively. The highest value of α_a is $3,5 \times 10^6$ at 1,49 eV. As seen in Figure 2a, the highest absorption was seen at 837 nm. With the effect of annealing, the highest absorption peak shifted from the visible to the infrared region. This caused the forbidden energy band gap to decrease to 1.15 eV, as seen in Figure 2d. In Figure 2c, the visible region boundaries at 400-700 nm are %11,02 and %10,35 percent transmittance values, respectively. The transmitance values of the film increased with annealing. This may be due to the absorption shift from the visible to the infrared region. The transmitance values of the glass/GaSe/InSe(annealed) thin film increased with annealing.
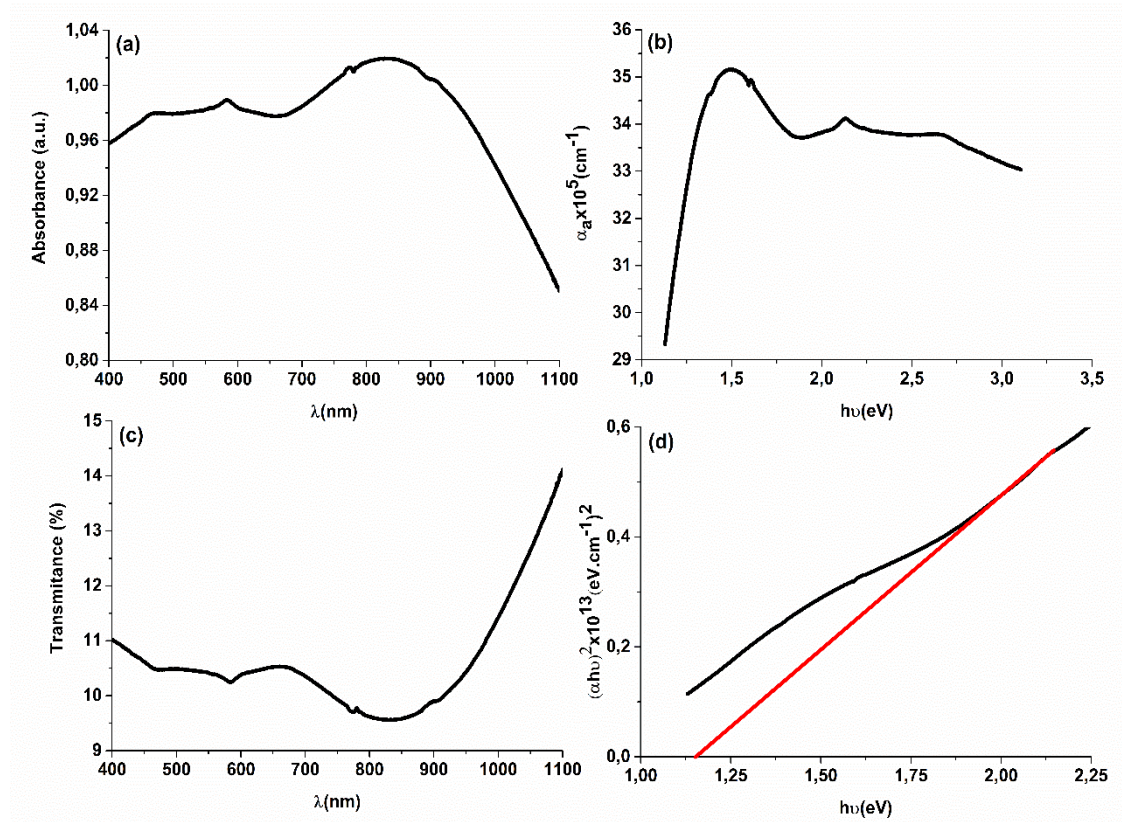
Figure 2. The optical spectrum of glass/GaSe/InSe(annealed) thin films: a) absorbance, b) absorbtion coefficient, c) transmittance and d) the photon energy dependence of $(\alpha h\upsilon)^2$.

3.2. Electrical Properties

The I-V characteristics of the as-deposited and annealed films were examined under dark and yellow light intensity 100 w/m². Figure 3a shows the schematic representation of the device produced, Fig 4a shows the current graph plotted against the voltage in the dark and light environment, and 4b shows the graphs of the junction resistance Rj ($Rj = \frac{\partial V}{\partial I}$) versus voltage.

In Figure 4a, it is seen that both as-deposited and annealed films are sensitive to light and their electrical conductivity increases under light. It is also seen that the photoconductivity of the as-deposited film is higher than that of the annealed film. The reason for this can be shown, as seen in the optical analysis, the shift of the maximum absorption peak from the visible to the infrared region, the decrease in the maximum absorption coefficient and the increase in the transmitance in the visible region. It is also seen that there are three different regions in Figure. 4a. The first region suggests a trap controlled space charge limited. The second region is the region of superquadratic behavior caused by low concentration charge carriers. In the second region, the trap filling mechanism is dominant. In the 3rd region, as the application voltage increases, all trap levels in the band gap of the semiconductor layer are filled. This suggests that most of traps are filled and contribution of free

carrier to electric filed becomes appreciable (Kumar, Jain et al. 2003, Yakuphanoglu 2008, Chaudhary, Kumar et al. 2019).
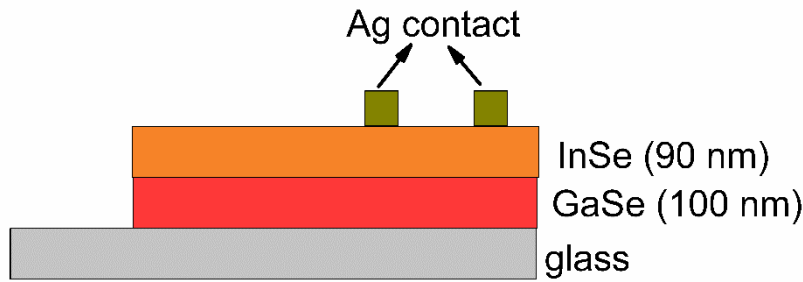

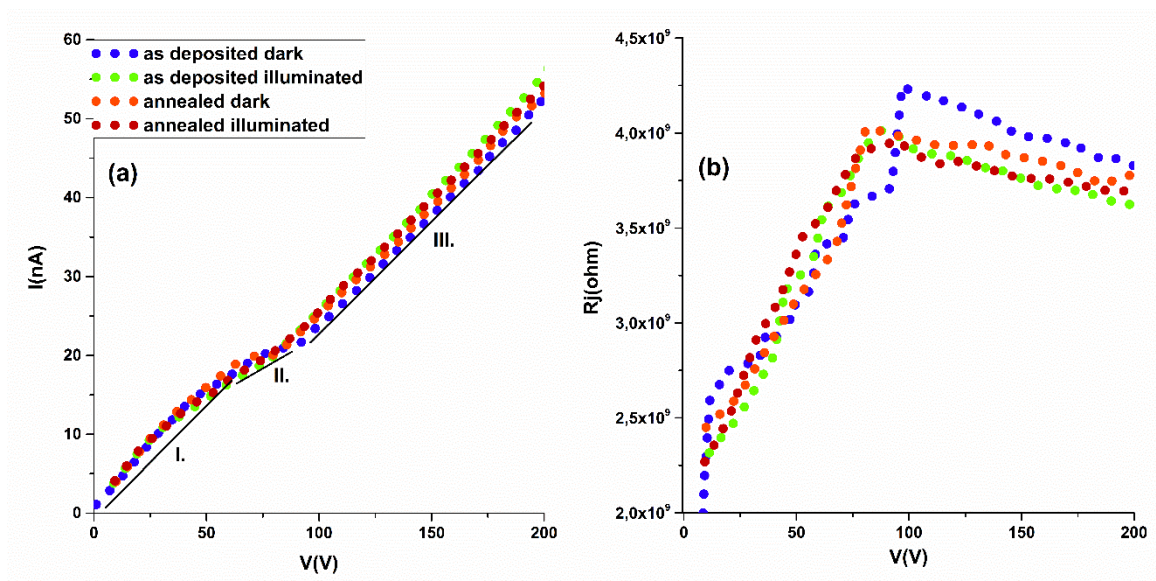**Figure 3.** Schematic representation of the fabricated device.

Figure 4. a) I-V characteristics of non-annealed and annealed devices, b) Rj-V characteristics of non-annealed and annealed devices

Figure 5a and b shows I-V and Rj-V graphs against temperature change, respectively. With the increase in temperature, the electrical conductivity increased with the decrease of Rj. In Figure 6a and b, graphs of resistivity and conductivity versus temperature are given at a constant potential, respectively. While the resistivity was determined as 0.7×10^9 (ohm.cm) at 285 °K, it was determined as 0.1×10^9 (ohm.cm) at 407 °K. The conductivity was determined as $1,3 \times 10^{-9}$ (ohm.cm)$^{-1}$ at 285 °K and $6,6 \times 10^{-9}$ (ohm.cm)$^{-1}$ at 407 °K. This is one of the biggest properties that distinguishes semiconductors from metals.
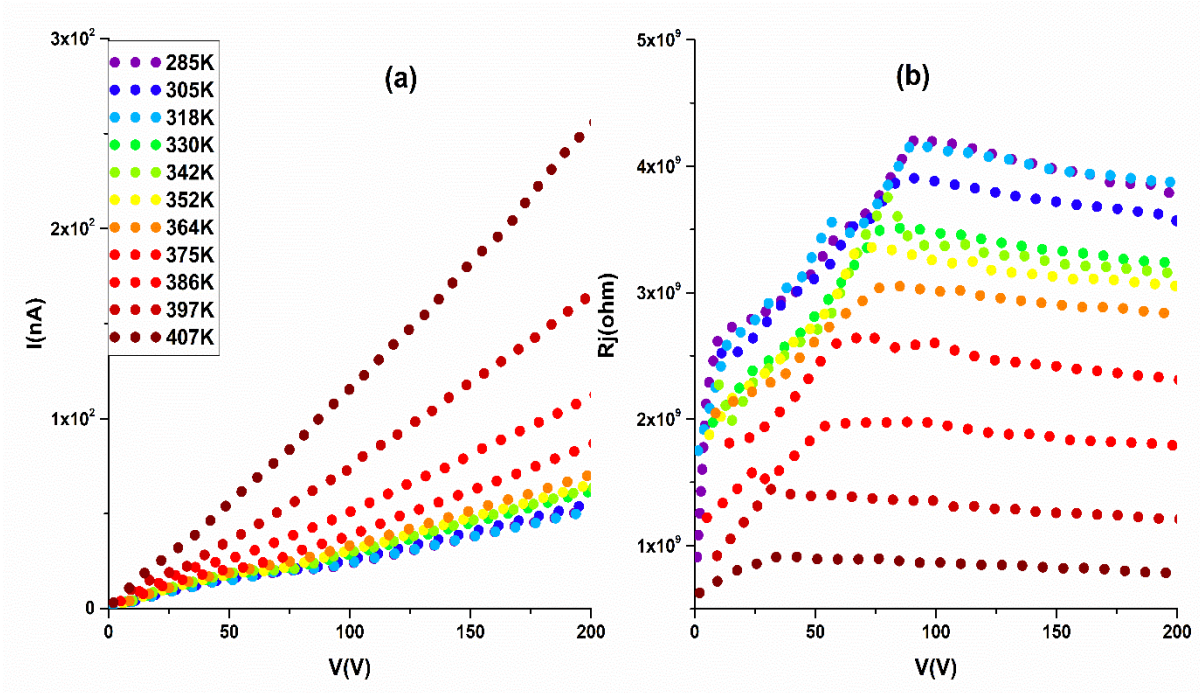
Figure 5. Temperature-dependent a) I-V characteristics, b) Rj-V characteristics of the as-deposited film.
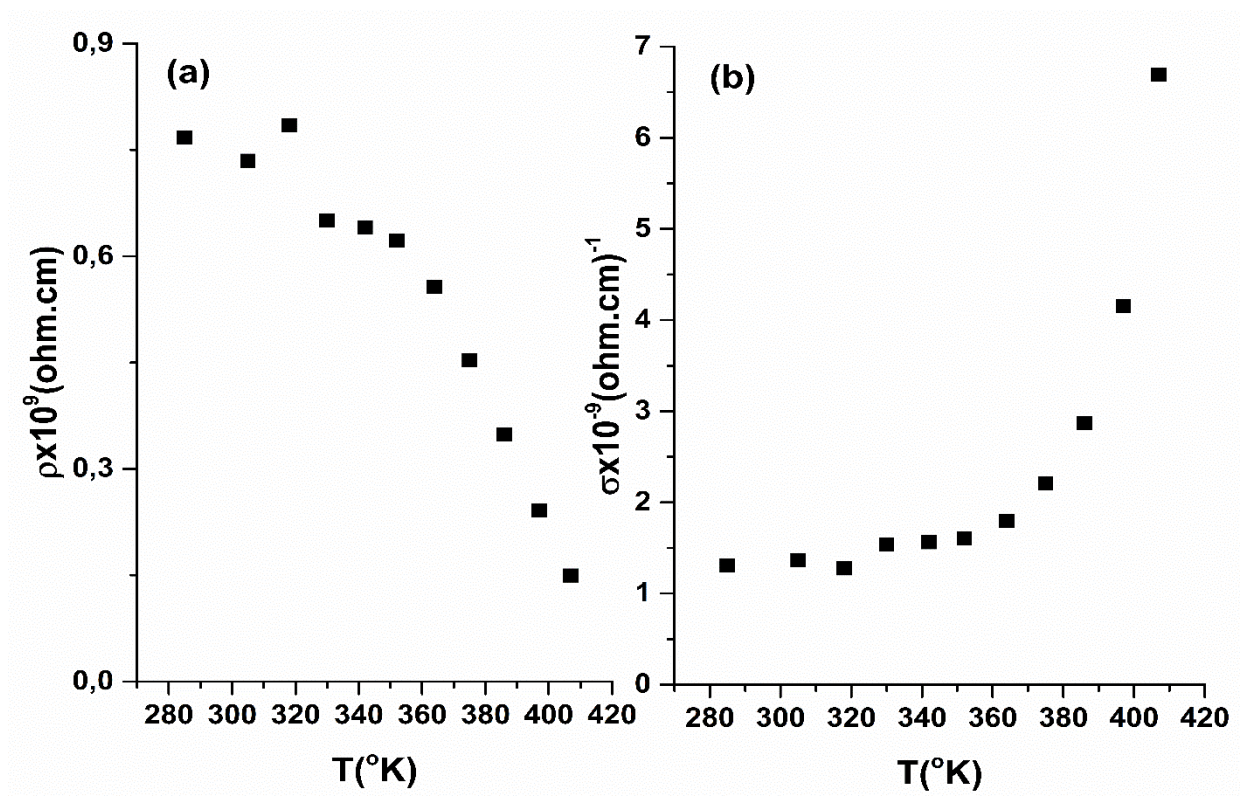

Figure 6. Temperature-dependent a) resistivity, b) conductivity of the as-deposited film.

,Also activation energies for as-deposited film were calculated within 285-407 °K temperature range and corresponding $\log\sigma$-10^3/T plots were recorded. The calculations were made according to following equation (Kobbi and Kesri 2004, Yilmaz 2008):

$$\sigma = \sigma_0 \exp(-\Delta E / kT) \tag{2}$$

The $\log\sigma$-10^3/T curve depicted in Figure 7 in this temperature range represent that the activation energy in low temperature region (285-342 °K) is 0,05 eV, it is 0,23 eV in middle temperature region (352-375 °K) while it is 0.6 eV in high temperature region (386-407 °K). The increment in conductance is non-linear owing to presence of amorphous structure of the film (Pathan, Kulkarni et al. 2005).
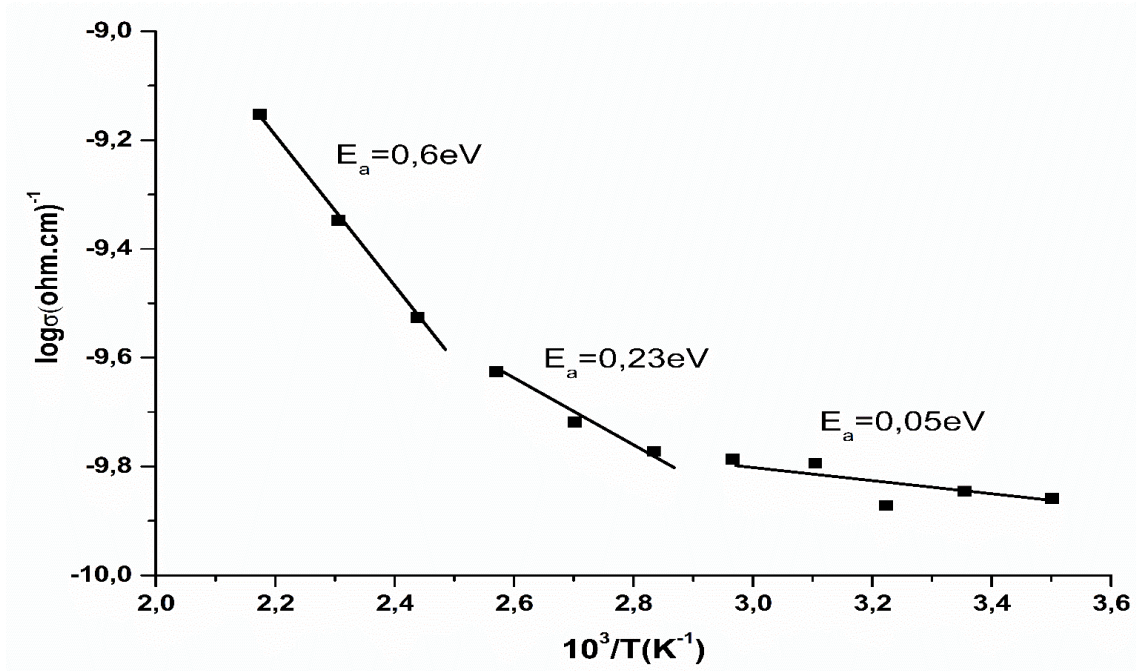

Figure 7. Arrhenius plot of the conductance of device (T = absolute temperature)

4. Conclusions and Recommendations

The InSe thin film was successfully grown on a glass/GaSe substrate using the M-CBD method and a group was annealed. While the energy band gap of the as-deposited film was 1.89eV, the energy band gap of the annealed film was determined as 1.15 eV. The maximum absorption region shifted from the visible to the infrared region by annealing. The as-deposited device is ideal for opto-electronic applications in the visible region, while the annealed film is ideal for applications used in

the infrared region. In addition, with annealing while the maximum absorption coefficient α_a decreased, optical transmittance and electrical conductivity increased.

The I-V characterization of the device at different temperatures was examined, the resistivity decreased and the conductivity increased with the increase of the temperature. The activation energy in low temperature region is 0,05 eV, while it is 0.6 eV in high temperature region.

Authors' Contributions

Fatih ÜNAL: Experimetal, Investigation, Formal analysis, Writing - review & editing.

Statement of Conflicts of Interest

There is no conflict of interest between the authors.

Statement of Research and Publication Ethics

The author declares that this study complies with Research and Publication Ethics.

References

Boukhvalov, D. W., B. Gurbulak, S. Duman, L. Wang, A. Politano, L. S. Caputi, G. Chiarello and A. Cupolillo (2017). "The Advent of Indium Selenide: Synthesis, Electronic Properties, Ambient Stability and Applications." Nanomaterials **7**(11).

Camara, M. O. D., A. Mauger and I. Devos (2002). "Electronic structure of the GaSe/Si(111) and InSe/Si(111) heterojunctions." Physical Review B **65**(20).

Camara, M. O. D., A. Mauger and I. Devos (2002). "Electronic structure of the layer compounds GaSe and InSe in a tight-binding approach." Physical Review B **65**(12).

Chaudhary, V., N. Kumar and A. K. Singh (2019). "Solubility dependent trap density in poly (3-hexylthiophene) organic Schottky diodes at room temperature." Synthetic Metals **250**: 88-93.

Choi, I. H. and P. Y. Yu (2003). "Properties of phase-pure InSe films prepared by metalorganic chemical vapor deposition with a single-source precursor." Journal of Applied Physics **93**(8): 4673-4677.

Dugan, S., M. M. Koç and B. Coşkun (2020). "Structural, electrical and optical characterization of Mn doped CdO photodiodes." Journal of Molecular Structure **1202**: 127235.

El-Sayed, S. M. (2003). "Optical investigations of the indium selenide glasses." Vacuum **72**(2): 169-175.

Gopal, S., C. Viswanathan, B. Karunagaran, S. K. Narayandass, D. Mangalaraj and J. Yi (2005). "Preparation and characterization of electrodeposited indium selenide thin films." Crystal Research and Technology **40**(6): 557-562.

Gopal, S., C. Viswanathan, M. Thamilselvan, K. Premnazeer, S. K. Narayandass and D. Mangalaraj (2004). "Conduction studies on electrodeposited indium selenide thin films." Ionics **10**(3-4): 300-303.

Han, G., Z. G. Chen, J. Drennan and J. Zou (2014). "Indium Selenides: Structural Characteristics, Synthesis and Their Thermoelectric Performances." Small **10**(14): 2747-2765.

Ho, C. H. and Y. J. Chu (2015). "Bending Photoluminescence and Surface Photovoltaic Effect on Multilayer InSe 2D Microplate Crystals." Advanced Optical Materials **3**(12): 1750-1758.

Igasaki, Y. and T. Fujiwara (1996). "The preparation of highly oriented InSe films by electrodeposition." Journal of Crystal Growth **158**(3): 268-275.

Jin-Ho Park, Mohammad Afzaal, Madeleine Helliwell, Mohmmad A. Malik, Paul O'Brien and J. Raftery (2003). "Chemical Vapor Deposition of Indium Selenide and Gallium Selenide Thin Films from Mixed Alkyl/Dialkylselenophosphorylamides." Chem. Mater. **15**: 4205-4210.

Julien, C., N. Benramdane and J. P. Guesdon (1990). "Transformation steps of structure in flash-deposited films of a-InSe." Semiconductor Science and Technology **5**(8): 905-910.

Julien, C., A. Chevy and D. Siapkas (1990). "Optical properties of In2Se3 phases." physica status solidi (a) **118**(2): 553-559.

Kobbi, B. and N. Kesri (2004). "Physico-chemical and electrical properties of InSe films." Vacuum **75**(2): 177-182.

Kumar, V., S. C. Jain, A. K. Kapoor, J. Poortmans and R. Mertens (2003). "Trap density in conducting organic semiconductors determined from temperature dependence of J-V characteristics." Journal of Applied Physics **94**(2): 1283-1285.

Lang, O., A. Klein, R. Schlaf, T. Löher, C. Pettenkofer, W. Jaegermann and A. Chevy (1995). "InSeGaSe heterointerfaces prepared by Van der Waals epitaxy." Journal of Crystal Growth **146**(1): 439-443.

Lokhande, C. D. and S. H. Pawar (1989). "Electrodeposition of Thin Film Semiconductors." physica status solidi (a) **111**(1): 17-40.

Mudd, G. W., S. A. Svatek, T. Ren, A. Patane, O. Makarovsky, L. Eaves, P. H. Beton, Z. D. Kovalyuk, G. V. Lashkarev, Z. R. Kudrynskyi and A. I. Dmitriev (2013). "Tuning the Bandgap of Exfoliated InSe Nanosheets by Quantum Confinement." Advanced Materials **25**(40): 5714-+.

Pathan, H. M., S. S. Kulkarni, R. S. Mane and C. D. Lokhande (2005). "Preparation and characterization of indium selenide thin films from a chemical route." Materials Chemistry and Physics **93**(1): 16-20.

Politano, A., D. Campi, M. Cattelan, I. Ben Amara, S. Jaziri, A. Mazzotti, A. Barinov, B. Gurbulak, S. Duman, S. Agnoli, L. S. Caputi, G. Granozzi and A. Cupolillo (2017). "Indium selenide: an insight into electronic band structure and surface excitations." Scientific Reports **7**.

Tauc, J. (1968). "Optical properties and electronic structure of amorphous Ge and Si." Materials Research Bulletin **3**(1): 37-46.

ÜNAL, F., T. İZGİ, B. BARIŞ and S. KARADENİZ (2020). "Cam/ITO/CIS/Rubrene Heteroekleminin Yüzey ve Optiksel Özelliklerinin İncelenmesi." Karadeniz Fen Bilimleri Dergisi **10**.

Yakuphanoglu, F. (2008). "Photovoltaic properties of the organic–inorganic photodiode based on polymer and fullerene blend for optical sensors." Sensors and Actuators A: Physical **141**(2): 383-389.

Yetim, N. K., N. Aslan, A. Sarıoğlu, N. Sarı and M. M. Koç (2020). "Structural, electrochemical and optical properties of hydrothermally synthesized transition metal oxide (Co3O4, NiO, CuO) nanoflowers." Journal of Materials Science: Materials in Electronics **31**(15): 12238-12248.

Yilmaz, S. (2008). "TETRAGONAL $(Bi_2O_3)_{1-x}(Ln_2O_3)_x$ İKİLİ SİSTEMLERİNDE İYONİK İLETKENLİĞİN İNCELENMESİ VE KATKI CİNSİNE BAĞLILIĞI (Ln=Dy, Eu, Sm)." Erciyes Üniversitesi Fen Bilimleri Enstitüsü Dergisi **24**: 212-215.

Yuksek, M., H. G. Yaglioglu, A. Elmali, E. M. Aydin, U. Kurum and A. Ates (2014). "Nonlinear and saturable absorption characteristics of Ho doped InSe crystals." Optics Communications **310**: 100-103.

Zhou, J., J. Shi, Q. Zeng, Y. Chen, L. Niu, F. Liu, T. Yu, K. Suenaga, X. Liu, J. Lin and Z. Liu (2018). "InSe monolayer: synthesis, structure and ultra-high second-harmonic generation." 2D Materials **5**(2).

Zhou, J. D., J. Shi, Q. S. Zeng, Y. Chen, L. Niu, F. C. Liu, T. Yu, K. Suenaga, X. F. Liu, J. H. Lin and Z. Liu (2018). "InSe monolayer: synthesis, structure and ultra-high second-harmonic generation." 2d Materials **5**(2).